

1 ***Frem2* Knockout Mice Exhibit Fraser Syndrome Phenotypes and Neonatal Lethality Due to Bilateral Renal** 2 **Agenesis**

3 Rubina G. Simikyan¹, Xinyuan Zhang¹, Olga Strelkova¹, Nathan Li², MengYu Zhu¹, Andreas Eckhard¹, Petr Y.
4 Baranov⁴, Xudong Wu³, Lauren Richey², Artur A. Indzhukulian¹.

5 1. Department of Otolaryngology Head and Neck Surgery, Mass Eye and Ear, Harvard Medical School, Boston,
6 MA, United States.

7 2. Tufts Comparative Medicine Services, Tufts University, Boston, MA, United States.

8 3. Department of Neurobiology, Harvard Medical School, Boston, MA, United States.

9 4. Schepens Eye Research Institute, Massachusetts Eye and Ear, Harvard Medical School, Boston, MA, United
10 States.

11 Correspondence should be addressed to inartur@hms.harvard.edu

12 **ABSTRACT**

13 Fraser syndrome is a rare autosomal recessive disorder characterized by multiple congenital malformations,
14 including cryptophthalmos, syndactyly, and renal agenesis, which can lead to severe complications beginning at
15 the embryonic stage. Mutations in genes encoding extracellular matrix proteins such as FRAS1, FREM1,
16 FREM2, and the associated trafficking protein GRIP1, are implicated in Fraser syndrome. These proteins are
17 critical for maintaining epithelial integrity during embryogenesis, with deficiencies leading to tissue detachment
18 and blistering phenotypes in mouse models. The FREM2 protein is a single-pass membrane protein of 3169
19 amino acids. While FREM2-deficient mouse models encoding missense variants found in patients, or a truncated
20 FREM2 protein product were previously reported, it has not been studied in a constitutive knockout (KO) mouse
21 model.

22 Here, we developed constitutive *Frem2*-KO mice exhibiting neonatal lethality, mainly due to bilateral renal
23 agenesis, along with blood-filled blisters, cryptophthalmos, and syndactyly. Only one mouse survived to
24 adulthood exhibiting unilateral renal agenesis and Fraser syndrome-like phenotypes. These findings confirm
25 FREM2's crucial role in the development of the kidneys, skin, and eyes and provide an animal model for further
26 studies of FREM2-related developmental disorders.

27 **INTRODUCTION**

28 Fraser syndrome is a rare autosomal recessive disorder characterized by developmental malformations evident
29 before birth (Smyth et al., 2005). Individuals affected may exhibit various features such as cryptophthalmos
30 (fused eyelids), syndactyly (fused fingers and toes), and unilateral or bilateral renal agenesis (failure of kidney
31 development), alongside respiratory and ear abnormalities (Slavotinek et al., 2002). Despite its rarity, Fraser
32 Syndrome may contribute to early-term miscarriages, mainly due to renal or pulmonary complications at the
33 embryonic stage (Smyth et al., 2005). Patients without life-threatening phenotypes can survive into adulthood
34 and may utilize surgical interventions to resolve skin malformations such as syndactyly.

35 FRAS1, FREM1, and FREM2 are structurally similar proteins shown to serve as important components of the
36 extracellular matrix (ECM) protein complex (Pavlakis et al., 2011). These proteins are predominantly localized in
37 the skin within the *sublamina densa* of basement membranes, playing a critical role in preserving epithelial-
38 mesenchymal integrity. A protein that has a role in trafficking the ECM proteins to their correct location, GRIP1,
39 which is crucial for mediating organ morphogenesis. Although it is not included in the ECM protein complex, it
40 was suggested to play an important role in maintaining the structural integrity of tissues (Takamiya et al., 2004).
41 Mutations in the *Fras1*, *Frem1*, *Frem2*, and *Grip1* genes cause epithelial detachment at the level of the
42 sublamina densa (Pavlakis et al., 2011, Takamiya et al., 2004).

43 Previous studies reported that human mutations to *Fras1*, *Frem2*, and *Grip1* are causative of Fraser Syndrome,
44 however mutations in *Frem1* alone do not induce the disorder (Short et al., 2007). Nonetheless, mutations in

45 these genes result in similar phenotypes. The severity of these phenotypes in patients, caused by deleterious
46 mutations in or the absence of ECM proteins and GRIP1 highlights their requirement for assembling basement
47 membranes across critical organs such as the skin, kidneys, testes, and trachea during embryogenesis (Pavlakis
48 et al., 2008). Mouse models have proven an excellent tool for investigating the roles of key proteins in embryonic
49 development and explaining their phenotypic correlations.

50 Previously reported mouse models carrying mutations in this group of genes have displayed mutual blistering
51 phenotypes, often referred to as 'bleb' mutants (Pavlakis et al., 2011). Loss of function in *Grip1* results in blistering
52 on the eyes of mice, mimicking the mutant strain for eye blebs (*eb*) (Short et al., 2007). Mutations of *Fras1* in
53 mice produces blebs (*bl*) on the paws. Mutations in *Frem1* cause head blebs (*heb*) in mice, often appearing as
54 blisters on the head along with absent or malformed eyes at birth (Smyth et al., 2004). Myelencephalic bleb (*my*)
55 mutant mice are related to the *Frem2* gene (Jadega et al., 2005). *Fras1*- and *Grip1*-knockout mouse models
56 were shown to display blistering phenotypes as early as 12-13 days of gestation and reported the deficiency of
57 the genes led to embryonic lethality (Bladt et al., 2002; Vrontou et al., 2003). Mutations of *Frem2* in mice have
58 reported cryptophthalmos, epithelial blebbing, blood-filled blisters, renal agenesis, and bony syndactyly (Jadega
59 et al., 2005; Zhang et al., 2019). Previously reported *Frem2* mouse models carry either point mutations
60 (*Frem2*^{R2156W} corresponding to a variant seen in a cryptophthalmos patient) or missense mutations (*Frem2*^{R725X},
61 *Frem2*^{my-F11}), and gene trap mutations (*my*^{Ucl}/*my*^{KST}) (Zhang et al., 2019; Timmer et al., 2005; Jadega et al., 2005).
62 To the best of our understanding, these animal models carry variants predicted to produce either a truncated
63 FREM2 protein, or one with a single amino acid substitution. These models are likely to result in milder
64 phenotypes, as these *Frem2* variants seem to induce FREM2 protein deficit mainly within certain cell types or
65 specific organs, such as the cryptophthalmos phenotype of the *Frem2*^{R725X/R2156W} mouse model (Zhang et al.,
66 2019). However, a constitutive *Frem2* knockout (KO) mouse model, lacking FREM2 expression throughout the
67 body, has not been carefully characterized.

68 To assess whether the absence of FREM2 recapitulates the reported phenotypes in *Frem2* mutants, or perhaps,
69 results in a more exacerbated phenotype, we developed and characterized a constitutive *Frem2*-KO mouse
70 model. Upon anatomical and histological analysis, we found that the *Frem2*-KO mice exhibit neonatal mortality
71 which we associate with bilateral renal agenesis. In addition, the *Frem2*-KO fetuses develop blood-filled blisters
72 on the eyes and paws that progress into hemorrhages and missing eyelids. A single *Frem2*-KO mouse survived
73 to adulthood and displayed unilateral renal agenesis while exhibiting syndactyly, cryptophthalmos, and
74 microphthalmia. Our findings confirm FREM2's role as an important protein for the formation of the skin, kidneys,
75 and eyes. This *Frem2*-KO mouse model provides a valuable tool for further, more detailed prenatal investigation
76 of its critical roles in organ development and underlying phenotypes resulting from its absence.

77 RESULTS

78 Genetic analysis of *Frem2*-KO mouse model

79 Mouse ES cell clones were purchased from the European Conditional Mouse Mutagenesis Program and used
80 to generate the *Frem2*^{tm1a(EUCOMM)Hmgu} mouse line carrying the knockout-first allele with conditional potential
81 (F2KCR allele) (Fig. 1A). First, the FRT-flanked Neo cassette was excised by crossing with a FLP deleted strain
82 to generate the conditional *Frem2*^{fl/fl} allele. Although the generated mouse line was designed to carry a floxed
83 *Frem2* allele to enable cell-type specific FREM2 functional studies (Fig. 1A), following several breeding steps
84 with pan-Cre and tissue-specific Cre lines (see *Methods*), we were unable to generate adult homozygous *Frem2*-
85 floxed mice. Upon further investigation of the mouse genetics, and the sequencing results of the insertion part
86 of the floxed-*Frem2* mouse, we discovered mutations within the targeted insertion site. These included two in-
87 frame insertions (27 bp and 30 bp) and one in-frame deletion (9 bp) (Fig. 1A). Subsequently, we analyzed the
88 open reading frame in exon 1 of the floxed *Frem2* allele. We identified a premature stop codon (Fig. 1B) within
89 the fused intron sequence downstream of exon 1 in the Floxed-*Frem2*, which likely results in a truncated FREM2
90 protein, converting the floxed-*Frem2* allele by design into a constitutive null allele. All animals evaluated in this
91 study were obtained from *Frem2*^{+/-} x *Frem2*^{+/-} crosses.

92 ***Frem2-KO mice have hemorrhagic blisters and skeletal malformations on their paws***

93 Upon our examination of fetuses (E13-16), we immediately observed the skin deficit phenotype on their paws,
94 in agreement with previous studies reporting *FREM2*'s critical role in epidermis development. Hemorrhagic
95 blisters were observed on the digits of *Frem2-KO* fetuses at E15 and E16 (**Fig. 2A** and **B**) and were often used
96 to phenotype them. To observe the postnatal development of the limbs, newborn *Frem2* pups were collected.
97 When we assessed blood-filled blisters on the digits of newborn *Frem2-KO* pups, they were still present but often
98 appeared dry (**Fig. 2C**, arrowheads).

99 In newborn *Frem2-KO* pups, most hind paws revealed soft tissue syndactyly, independent of whether any blisters
100 were observed. Affected paws often also display dorsal flexure, an anatomical malformation where the paws curl
101 upwards (**Fig. 2D**). We next assessed the skeletal formation of the paws and other morphological features using
102 histological sections, which were carried out using the same orientation across all samples (**Fig. 2E**). We
103 determined that newborn *Frem2-KO* mice with paws that had blood-filled blisters, syndactyly, or dorsal flexure
104 also exhibited skeletal malformations at the digits, with the skeletal structure around them often compromised.
105 Interestingly, these regions of skeletal malformations typically occurred bilaterally on the hind limbs.

106 ***FREM2 deficiency causes ocular abnormalities in Frem2-KO mice***

107 We often observed even larger blood-filled blisters over the eyes of *Frem2-KO* fetuses. At E13, the *Frem2-KO*
108 fetuses can be identified by the pronounced bubble-like blisters over their eyes. Coronal head histology sections
109 of E15 *Frem2-KO* fetuses revealed blisters localized near or within the eyelids (**Fig. 3B** and **C**). In some cases,
110 the eyelids in *Frem2-KO* fetuses were thinned and hemorrhaged (**Fig. 3D** and **E**). Such hemorrhages and blood-
111 filled blisters appeared bilaterally or unilaterally on the eyelids of *Frem2-KO* fetuses (**Fig. 3E**).

112 In newborn *Frem2-KO* pups, however, no blood-filled blisters were observed. Instead, *Frem2-KO* pups
113 predominantly displayed missing eyelids, with some hemorrhages often observed on the skin around the eyes
114 (**Fig. 3F**). The heads of newborn pups were sectioned coronally to assess eye morphology using standard
115 histology techniques. In wild-type and heterozygous *Frem2* pups, the epidermal layers of the eyelids were
116 properly formed (**Fig. 3G**). In *Frem2-KO* pups, however, the eyelids were often missing (**Fig. 3H** and **I**) or
117 thinned (**Fig. 3I** and **J**). Periocular hemorrhages and the absence of eyelids were bilateral or unilateral in
118 *Frem2-KO* pups. Blood-filled blisters on the eyelids that occur during embryonic stages, as well as the missing
119 eyelids in newborn *Frem2*-deficient animals, suggest that proper *FREM2* expression is critical for the epidermal
120 development of the eyelids.

121 ***Frem2-KO mice die hours after birth***

122 During routine genotyping of *Frem2* litters, no *Frem2-KO* mice were identified. Interestingly, the dam was
123 observed giving birth to pups exhibiting phenotypes we observed in *Frem2-KO* embryos. However, a few hours
124 after birth, the pups were discovered dead in the cage. We thus concluded that *Frem2-KO* pups do not survive
125 after birth, and next sought to investigate the causes of this mortality. Multiple histological sections and post-
126 mortem necropsies were performed in newborn *Frem2-KO* pups. In almost all newborn *Frem2-KO* pups we
127 observed bilateral renal agenesis (**Fig. 4**). Likely a result of the lack of urine production from renal agenesis,
128 *Frem2-KO* pups had empty urinary bladders. We also commonly observed the absence of one or both adrenal
129 glands (**Fig. 4A** and **B**). Parasagittal sections further confirmed the renal agenesis and the empty urinary bladder
130 in newborn *Frem2-KO* pups (**Fig. 4C-F**). We carried our serial transverse histological sections to gain better
131 confidence in our macroscopic results (**Fig. 5** and **Supplementary Movies**). All *Frem2-KO* pups, but one, had
132 bilateral renal agenesis, confirmed by the necropsies or with histological evaluation. A single newborn *Frem2*-
133 *KO* pup displayed one small but developed kidney, confirming unilateral renal agenesis (**Fig. 5D**). *Frem2-KO*
134 pups also had empty urinary bladders. No major defects in other vital organs, such as the lungs and heart, were
135 seen in *Frem2-KO* pups upon examination with necropsy or histological analysis. We conclude that the likely
136 cause of postnatal mortality of *Frem2-KO* pups is the renal agenesis.

137 **A single case of *Frem2*-KO mouse surviving into adulthood**

138 Over the years of breeding, only one female *Frem2*-KO mouse survived until adulthood during this study.
139 Although no apparent health conditions were determined and the animal produced two litters, the female was
140 euthanized at the age of 51 weeks due to ulcerative dermatitis, common in older mice. Interestingly, the mouse
141 had displayed physical phenotypes, such as unilateral cryptophthalmos (**Fig. 6A**). The left eye of the mouse was
142 closed, with no visible eyelid crease. The contralateral eye, however, appeared normal. A post-mortem incision
143 through the skin of the closed eyelid, a significantly smaller eyeball was identified and sent for histological
144 analysis along with the contralateral eye. The histological analysis revealed a normally developed right eye and
145 a malformed left eye (**Fig. 6B**). The left eye was dramatically smaller in size, and the retina appeared to have
146 folds, often observed in microphthalmia (**Fig. 6B'**).

147 Consistent with our observations in newborn *Frem2*-KO mice, the front paws of the adult mouse appeared normal
148 (**Fig. 6C**), while both hind paws were affected by syndactyly (**Fig. 6D and E**). The hind paws were also slightly
149 curled, similar to the paws observed in newborns. We next examined the renal system of this adult mouse and
150 found that it had one functional kidney. There was no gross evidence of renal tissue on the right side (**Fig. 6F**).
151 The left kidney was fully attached to the ureter along with the rest of the urinary system. Hematoxylin and eosin
152 histological sections of the left kidney confirmed normal morphology of the adrenal gland and kidney (**Fig. 6G**).
153 Higher magnification images of the histological sections reveal apparently the normal histology of the adrenal
154 gland, as well as of the kidney, containing the normal appearance of tubules and nephrons (**Fig. 6H**). The
155 histological evaluation also showed a missing right ureter (**Fig. 6I**). Although missing a kidney, the reproductive
156 functions were not affected in the *Frem2*-KO female, allowing it to breed and produce litters. In the right uterine
157 horn, a placenta-like tissue was found (**Fig. 6I**). The renal pelvis was also dilated, according to gross examination.
158 As a result of the functional kidney, the urinary bladder was full (**Fig. 6K**). Although this female was able to
159 survive with one functional kidney, the *Frem2*-KO adult mouse displayed other prominent Fraser Syndrome
160 phenotypes, such as cryptophthalmos and syndactyly (**Fig. 6A, C and D**).

161 **DISCUSSION**

162 In this study, we developed a constitutive knockout (KO) *Frem2* mouse model to evaluate the associated
163 phenotypes. Our findings reveal that the absence of the FREM2 protein results in significant Fraser Syndrome-
164 like phenotypes, including cryptophthalmos, syndactyly, and blood-filled blisters, observable as early as during
165 the embryonic stage. *Frem2*-KO pups could be easily identified in litters due to their obvious phenotypes, even
166 before confirming their genotypes. Although *Frem2*-KO mice can survive until birth, they die shortly thereafter
167 likely due to bilateral renal agenesis. To date, only one *Frem2*-KO mouse with unilateral renal agenesis from our
168 animal colony has survived into adulthood. These results highlight the critical role of FREM2 in the development
169 of the epidermis, eyes, skeletal structure, and kidneys.

170 The extracellular matrix (ECM) is well-known for its role in providing structural support. However, it also plays a
171 crucial role in maintaining tissue integrity by regulating cell proliferation, differentiation, and survival. Specifically,
172 the ECM includes basement membranes that form sheets underlying epithelial and endothelial cell layers.
173 FREM2 is localized within the epithelial basement membrane. Previous studies using immunogold labeling have
174 demonstrated the clustered localization of FREM2 within the *sublamina densa* of embryonic skin, highlighting its
175 importance in tissue integrity (Pavlakakis et al., 2011). Mouse models with a deficiency of ECM proteins, such as
176 FREM2, reveal how disruptions in ECM components can lead to blistering phenotypes, highlighting the intricate
177 relationship between genetic mutations and the assembly of essential basement membranes (Petrou et al.,
178 2008). Unfortunately, our attempts to label FREM2 using several commercially available antibodies were not
179 successful.

180 Our observations support previously reported evidence from other studies that use *Frem2* mouse models in
181 reporting that mutations in *Frem2* can cause blood-filled blisters and hemorrhages on the skin. For instance, in
182 a study involving a *Frem2* mouse model of the *my^{Ucl}* strain, homozygote mutant mice exhibited epithelial blebbing
183 beginning at E11.5 (Jadeja et al., 2005). By E14, these blebs had progressed into hemorrhagic lesions. Another

184 study focused on embryonic development suggests that the onset of angiogenesis, the process of new blood
185 vessel formation involving the growth and differentiation of endothelial cells, may explain the timing of these
186 hemorrhages (Timmer et al., 2005). Inadequate adhesion of endothelial cells to adjacent structures, particularly
187 in cells deficient in *FREM2* protein, could explain deficits in angiogenesis (Timmer et al., 2005). Although *FREM2*
188 is not directly localized within vascular structures, and instead was located in the membrane that lines the blood
189 vessels, its role in stabilizing blood vessels during development appears critical (Timmer et al., 2005). The
190 absence of *FREM2* in surrounding tissues likely contributes to the hemorrhages observed on the skin which
191 aligns with the parallel occurrence of syndactyly and blood-filled blisters observed on the paws and eyes of
192 *Frem2-KO* mice. This further supports the conclusion that *FREM2* is essential not only for vascular stability but
193 also for tissue remodeling and skeletal development during gestation. However, the potential relationship
194 between these anomalies remains speculative, necessitating further experimental investigation to explain the
195 precise mechanisms involved.

196 Patients with Fraser Syndrome who exhibit cryptophthalmos are born with skin covering their eyes or with fused
197 eyelids. Instead in *Frem2*-deficient mice, this phenotype more often presents as the absence rather than the
198 fusing of eyelids. We observed that *Frem2-KO* fetuses developed blood-filled blisters or hemorrhages that cover
199 their eyes and give way to one or both eyelids' absence at birth. A study on *Frem2* mice carrying the *my^{F11}*
200 mutation, which is predicted to result in a truncated protein, indicated that embryonic hemorrhages might lead to
201 localized tissue necrosis, which could explain the absence of eyelids (Timmer et al., 2005). Given the proposed
202 role of *FREM2* in vascular stability, it is likely that the loss of *FREM2* during key morphogenic events, like eyelid
203 development, could lead to such hemorrhages. The subsequent blood-filled blisters and hemorrhages likely
204 inhibit normal skin development, causing the observed phenotypes.

205 Moreover, a study utilizing a compound heterozygous mutation derived from a Fraser Syndrome patient to
206 generate mice that mimic the human cryptophthalmos phenotype found significant abnormalities in eyelid
207 development during the critical stages at E13-14 (Zhang et al., 2021). Specifically, the lower eyelid fold was
208 poorly defined in *Frem2* mutant fetuses, in contrast to normal mice, where the grooves of the ectoderm that
209 eventually form the upper and lower eyelids are visible. These mutants exhibited dysplasia and microphthalmia,
210 with reductions in the eye's axial length and lens thickness. Eyes affected by microphthalmia typically have a
211 thicker cornea, an absent or severely underdeveloped lens, and a retina prone to folding or filling the vitreous
212 body. These features likely exert pressure on the lens, potentially exacerbated by the presence of blisters or
213 hemorrhages (Graw et al., 2019). In our *Frem2-KO* model, we observed microphthalmia where one eye was
214 smaller than the other, as well as retinal folding. In Fraser Syndrome patients, these ocular abnormalities often
215 lead to impaired vision. This shows that *FREM2* is not only important for eyelid development but also specifically
216 for eye development.

217 *FREM2* protein was reported to be expressed in the epithelia in the renal cortex, or the outer layer, of mouse
218 kidneys (Kerecuk et al., 2012). *FREM2* expression begins in the ureteric epithelia of the metanephros at E11.5,
219 with peak expression at the tips of the ureteric buds (Jadeja et al., 2005). In adult mice, *FREM2* is strongly
220 expressed in the collecting ducts, proximal convoluted tubules, and arterioles within the kidneys (Jadeja et al.,
221 2005). This expression pattern, along with the development of renal cysts in *Frem2* mutant animals, suggests
222 that *FREM2* is essential for maintaining renal integrity (Kerecuk et al., 2012). The absence of kidneys in *Frem2*-
223 *KO* mice that fail to survive postnatally provides additional evidence of *FREM2*'s critical involvement in renal
224 development. Interestingly, over multiple years of breeding, the only *Frem2-KO* mouse that survived into
225 adulthood had one functional kidney, suggesting that perhaps while *FREM2* is critical for renal development, it
226 is not absolutely indispensable. This partial necessity may be due to protein-protein interactions within the ECM
227 protein complex, where other proteins such as *FREM1* or *FRAS1* may, at least partially, compensate for the loss
228 of *FREM2* in the formation of the basement membrane. Although Fraser Syndrome is associated with a risk of
229 miscarriage, bilateral renal agenesis is a significant phenotype contributing to this, while patients with unilateral
230 renal agenesis can survive with a single kidney (Smyth et al., 2005). Since kidneys contribute to the amniotic
231 fluid in humans, by the second trimester of pregnancy, low amniotic fluid levels serve as an important indicator
232 of renal agenesis in the fetus (Miller et al., 2023). Insufficient amniotic fluid, also known as oligohydramnios, in
233 addition to the absence of kidneys, poses a significant risk for fetal death. In contrast, the impact of bilateral renal
234 agenesis is markedly different in mice, resulting in death within 2 days after birth (Kamba et al., 2001). While the

235 mouse phenotype we observed in our *Frem2-KO* mice is clearly more severe when compared to other previously
236 reported *Frem2* mouse lines, given the uncertain rate of miscarriages related to *FREM2* dysfunction, it is difficult
237 to directly compare the severity of the phenotype we observed to that of patients carrying pathogenic *FREM2*
238 variants.

239 In summary, to address the gap in Fraser Syndrome research, we have developed and characterized a
240 constitutive *Frem2-KO* mouse model that lacks the *FREM2* protein. While previous studies have utilized various
241 *Frem2* mouse models, some of which have retained limited *FREM2* function, here we report a mouse model
242 predicted to lack *FREM2* entirely. Our findings reveal that *Frem2-KO* pups die shortly after birth, limiting the
243 opportunity for extensive study. Nevertheless, we have identified the most prominent phenotypes and the primary
244 cause of neonatal mortality. We acknowledge the possibility of non-morphological phenotypes, particularly in the
245 respiratory or cardiovascular systems, that have yet to be uncovered. Our study provides a unique, though
246 severe, model of Fraser Syndrome that can be utilized in future embryonic studies to advance the understanding
247 of Fraser Syndrome's pathophysiology. Critically, our work can help tease apart the crucial role the *FREM2* has
248 in the development of important organs and also in uncovering the underlying mechanisms that drive Fraser
249 Syndrome.

250 MATERIALS AND METHODS

251 *Animals*

252 Mouse ES cell clones (*Frem2*^{tm1a(EUCOMM)Hmgu}; clones HEPD0988-1-E06 and HEPD0988-1-H08) were purchased
253 from the European Conditional Mouse Mutagenesis Program (<https://www.mousephenotype.org/about-impcc/about-ikmc/eucomm/>, Clone# HEPD0988_1_E06, HEPD0988_1_H08). The clones were then used to
254 generate the *Frem2*^{tm1a(EUCOMM)Hmgu} mouse line carrying the knockout-first allele with the conditional potential
255 (F2KCR allele) (**Fig. 1A**) at the Harvard Transgenic Animal Core. For clone HEPD0988-1-E06, 36 blastocysts
256 were injected, 8 pups were born (5 died), and no chimera pups obtained from this injection. For clone HEPD0988-
257 1-H08, 48 blastocysts were injected, 15 pups were born (5 died), and two of the 10 surviving pups were chimeric
258 mice (1 male was 15% and 1 female was 40% chimeric). The two chimera mice were bred to get germline
259 transmission. The founder mice were then imported to the Mass Eye and Ear animal facility to set up an animal
260 colony. To generate the conditional *Frem2*^{fl/fl} allele the FRT-flanked Neo cassette was excised by crossing with
261 a FLP deleter strain (The Jackson Laboratory, #003946).

262 The *knockout-first* mouse line (*Frem2-KO-first* allele with conditional potential, F2KCP) derived from these ES
263 cells contains an "FRT-Exon2-LacZ-LoxP-NeoR-FRT-LoxP-Exon3-LoxP" cassette in the middle of exon 1 of the
264 wildtype *FREM2* gene. We found that the exon 2 named in the vendor's sequence is not present in the other
265 published *FREM2* wildtype gene (Ensembl.org). The F2KCR line was bred with the FLP mouse (Jax Cat#
266 003946) to delete the "FRT-Exon2-LacZ-LoxP-NeoR" part and obtain a floxed *FREM2* line containing "Exon1-
267 FRT-LoxP-Exon3 (or Exon1b)-LoxP" structure.

268 All procedures and protocols were approved by the Institutional Animal Care and Use Committee of Mass Eye
269 and Ear and we have complied with all relevant ethical regulations for animal use. All mice were kept on a 12:12
270 hour light-dark cycle with unlimited access to food and water. The fetuses were collected by timed breedings or
271 by keeping track of the pregnancy by weighing the dam. For the collection of newborn pups, the breeding cages
272 with pregnant females were closely monitored for litter birth by an infrared webcam setup below the cage with a
273 remote access functionality.

274 *Phenotypic Analysis and Fixation of Fetuses*

275 Mouse fetuses were collected by euthanizing pregnant adult females at the needed gestation stage. Fetuses
276 were collected and fixed in Bouin's fixative (Electron Microscopy Sciences). E12.6-16.5 were fixed for 4 hours.
277 E17.5-18.5 were fixed for 72 hours. The fetuses were then rinsed in three changes of 70% alcohol and stored at
278 70% alcohol until processing.

280 **Collection and Fixation of Newborn Pups**

281 Newborn mouse pups were collected at P0 once the litter was detected using an infrared webcam setup (ELP
282 1080p USB Camera). Pups were cryoanesthetized, weighed, imaged, and the tip of the tail was collected for
283 genotyping. Pups were then euthanized by decapitation and fixed in Bouin's solution (Electron Microscopy
284 Sciences, Cat# 15990-01) for 72 hours. After fixation, samples were rinsed in three changes of 70% alcohol and
285 stored at 70% alcohol until processing. Pups used for gross anatomy evaluation were euthanized, and a median
286 laparotomy was done from the pubic crest to the trachea.

287 **Histology**

288 Fetal and newborn pup bodies were trimmed into three sections with cuts at the diaphragm and pelvis to ensure
289 adequate paraffin embedding and tissue processing. Heads were trimmed for coronal embedding to the area of
290 interest. Samples were processed using a Microm STP-120 processor on a routine program for manual paraffin
291 embedding with a Microm EC-350 embedding center. After paraffin embedding, 5µm sections were cut from the
292 head and body for Hematoxylin and eosin staining. Sections from the bodies were collected distally every ~400
293 µm through the entire cavity. Slides were imaged with the Aperio AT2 automatic slide scanner (Leica Biosystems)
294 using a 0.5x objective lens and processed with the Aperio ImageScope software.

295 **ACKNOWLEDGEMENTS**

296 We would like to thank Dr. David Corey for developing the *Frem2-KO* mouse line; Philip Seifert and the Schepens
297 Eye Research Institute Morphology Core for sectioning eye samples for histology; Sarah Visconti for assistance
298 in breeding and imaging mice; Dr. Frank Yeh for providing edits and critical feedback to the manuscript. This
299 work was supported by NIH R01DC020190 (NIDCD) and R01DC017166 (NIDCD) to A.A.I. The funder had no
300 role in study design, data collection and analysis, decision to publish, or preparation of the manuscript.

301 **DATA AVAILABILITY**

302 All data are included within the manuscript or are available upon request. All imaging data will be made available
303 from a public data repository upon acceptance of the manuscript for publication.

304 **COMPETING INTERESTS**

305 The authors declare no competing interests.

306 **AUTHOR CONTRIBUTIONS**

307 **RGS:** Validation, Formal Analysis, Investigation, Writing – Original Draft, Writing – Review & Editing,
308 Visualization, Project administration.

309 **GZ:** Validation, Formal Analysis, Investigation, Writing – Review & Editing.

310 **OSS:** Validation, Formal Analysis, Investigation, Writing – Review & Editing.

311 **NL:** Investigation, Resources, Writing – Review & Editing.

312 **MZ:** Resources, Writing – Review & Editing, Visualization.

313 **AE:** Resources, Writing – Review & Editing.

314 **PYB:** Validation, Resources, Writing – Review & Editing.

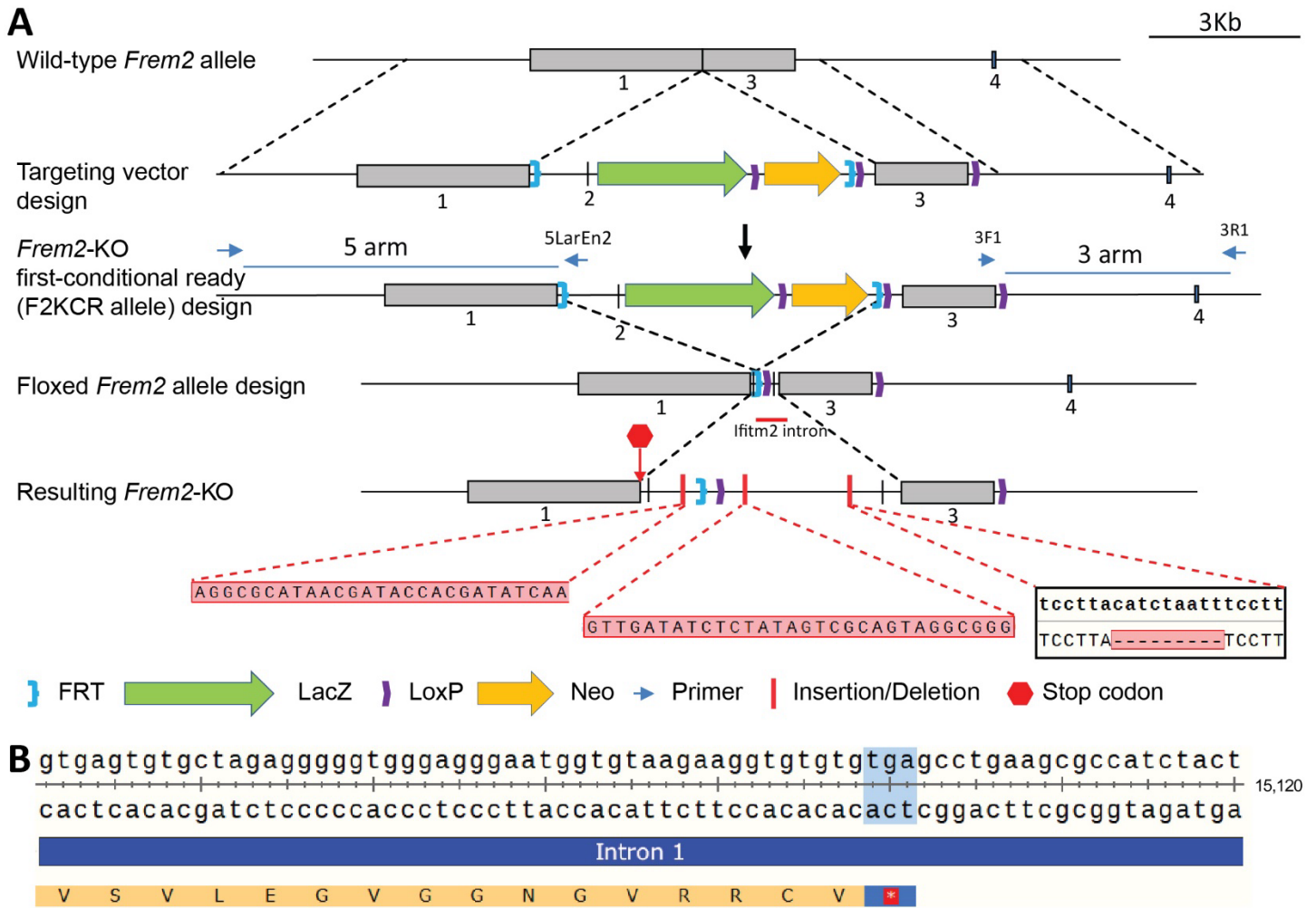
315 **SW:** Conceptualization, Methodology, Validation, Formal Analysis, Investigation, Writing - Review & Editing,
316 Visualization.

317 **LR:** Methodology, Validation, Investigation, Resources, Writing – Review & Editing, Supervision.

318 **AAI:** Conceptualization, Methodology, Validation, Formal analysis, Investigation, Resources, Visualization,

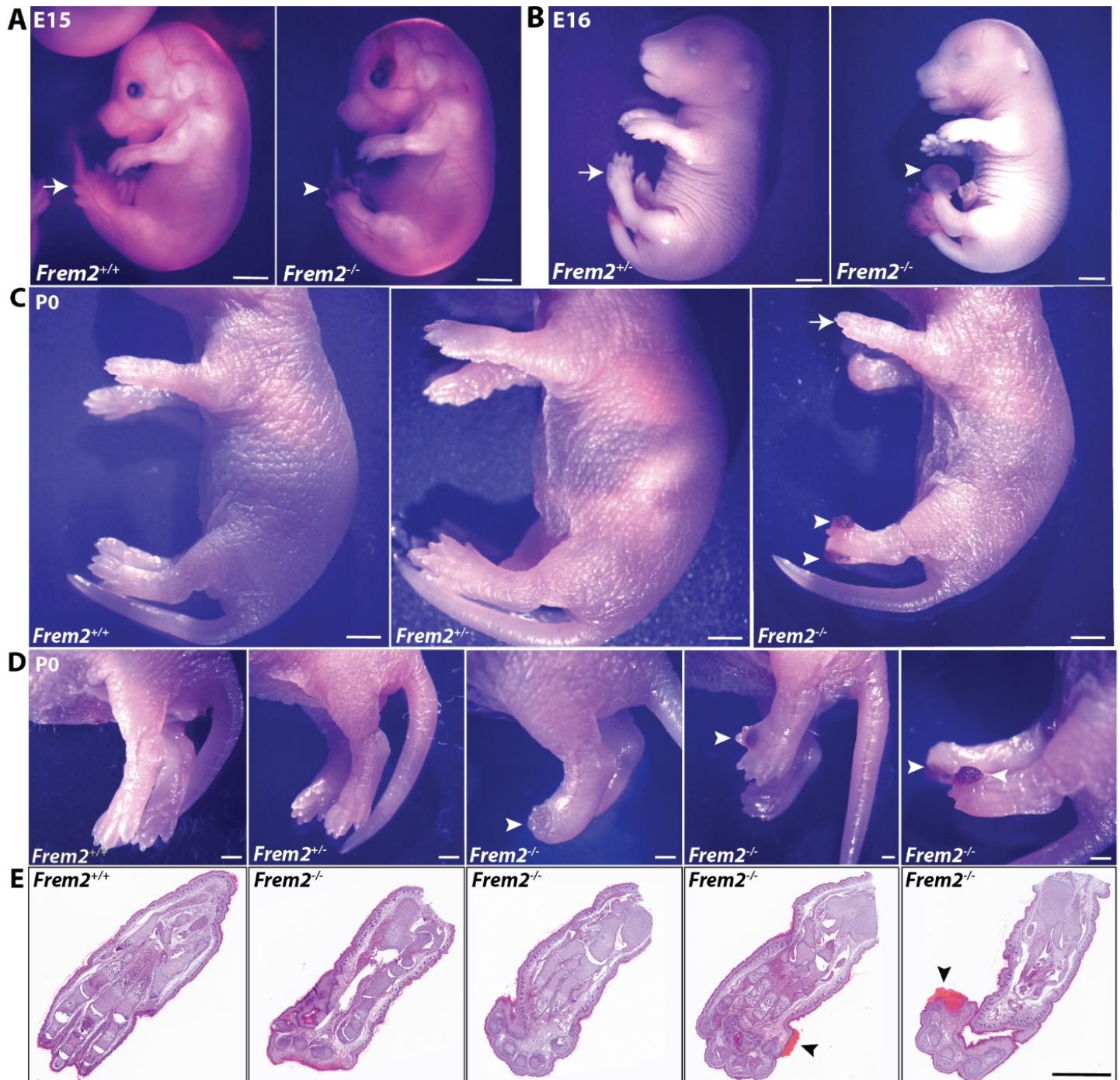
319 Writing – Original Draft, Supervision, Project administration, Funding acquisition.

320 **FIGURES**



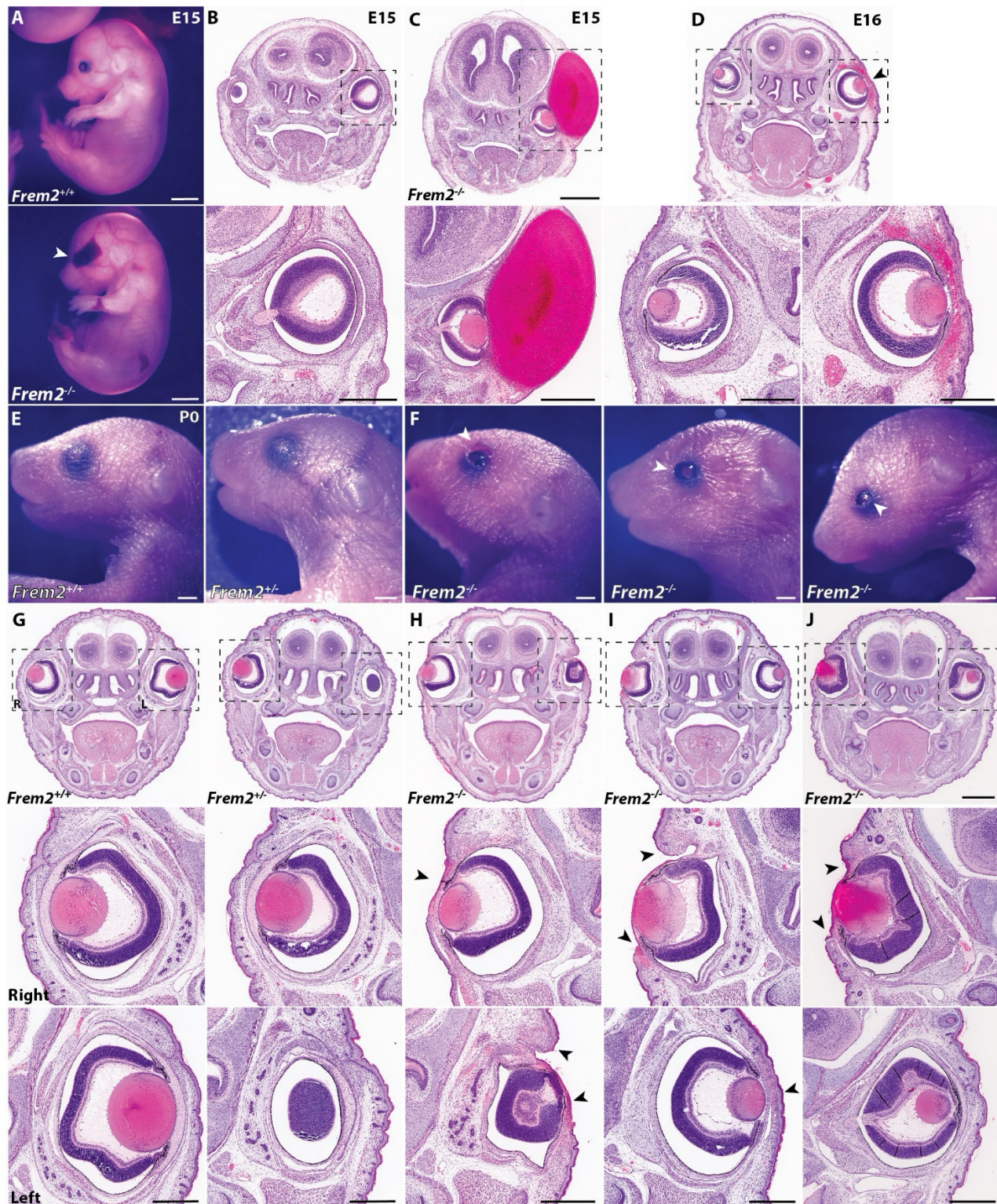
321

322 **Figure 1. *Frem2*-KO mouse design strategy.** **A**, ES cells with a *Frem2*-KO-first conditional ready allele were used to
 323 generate the Floxed-*Frem2* mouse line. The floxed allele shows exon 2 deleted as a result of the FLP and FRT system. The
 324 conditional-KO mouse displays the in-frame mutations (shown as a red line) and their sequences: two insertions (27 bp and
 325 30 bp) and one deletion (9 bp). **B**, A portion of the sequence (15100-15120 bp) for exon 1 of Floxed-*Frem2* is displayed.
 326 The premature TGA stop codon sequence is highlighted in blue near the middle of the reading frame.

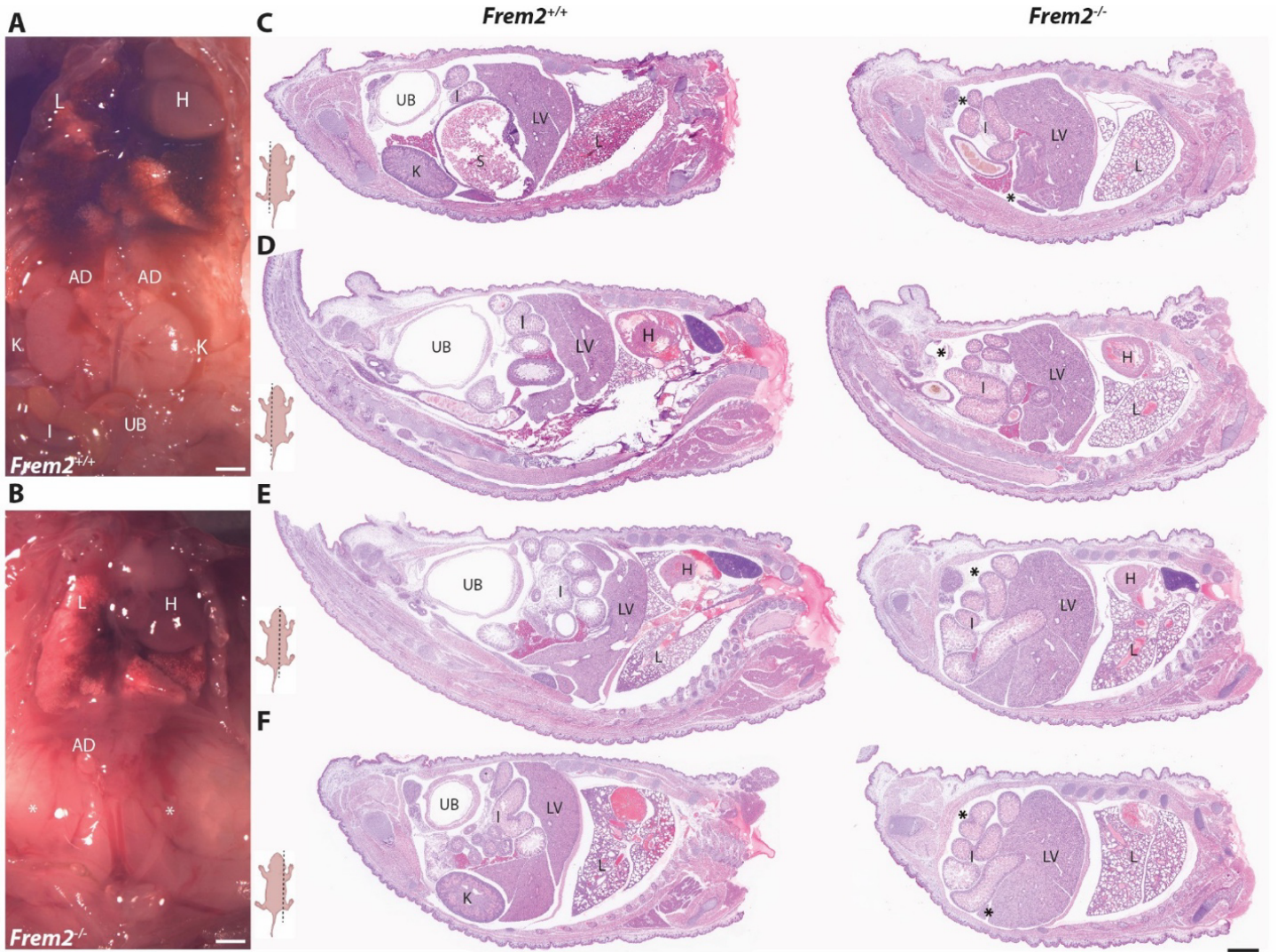


327

328 **Figure 2. *Frem2*-KO fetuses and newborn pups exhibit hemorrhagic blisters and syndactyly.** **A**, *Frem2*^{+/+} (wild-type)
329 E15 fetus (left) with normal paws (arrow) and a *Frem2*^{-/-} (KO) littermate (right) with a blood-filled blister over the digits
330 (arrowhead). **B**, E16 heterozygous *Frem2*^{+/-} fetus (left) with normal paws (arrow) and E16 *Frem2*^{-/-} fetus littermate (right)
331 with a large hemorrhagic bleb on the digits (arrowhead). **C**, P0 *Frem2*^{+/+} (left) and *Frem2*^{+/-} (middle) have normal paws, and
332 a *Frem2*^{-/-} (right) has dried blood-filled blisters on both hind paws. **D**, Newborn *Frem2*^{-/-} pups with a malformation of hind
333 limbs, soft-tissue syndactyly, and blood-filled blisters on digits. Reference *Frem2*^{+/+} and *Frem2*^{+/-} paws showing normal paw
334 morphology. **E**, Hematoxylin and eosin-stained histology section of paws from wild-type (*Frem2*^{+/+}) and several knockout
335 (*Frem2*^{-/-}) mice with limb malformation and blood-filled blisters (arrowhead). Scale bars: (A)-(C): 2 mm, (D, E): 1 mm.

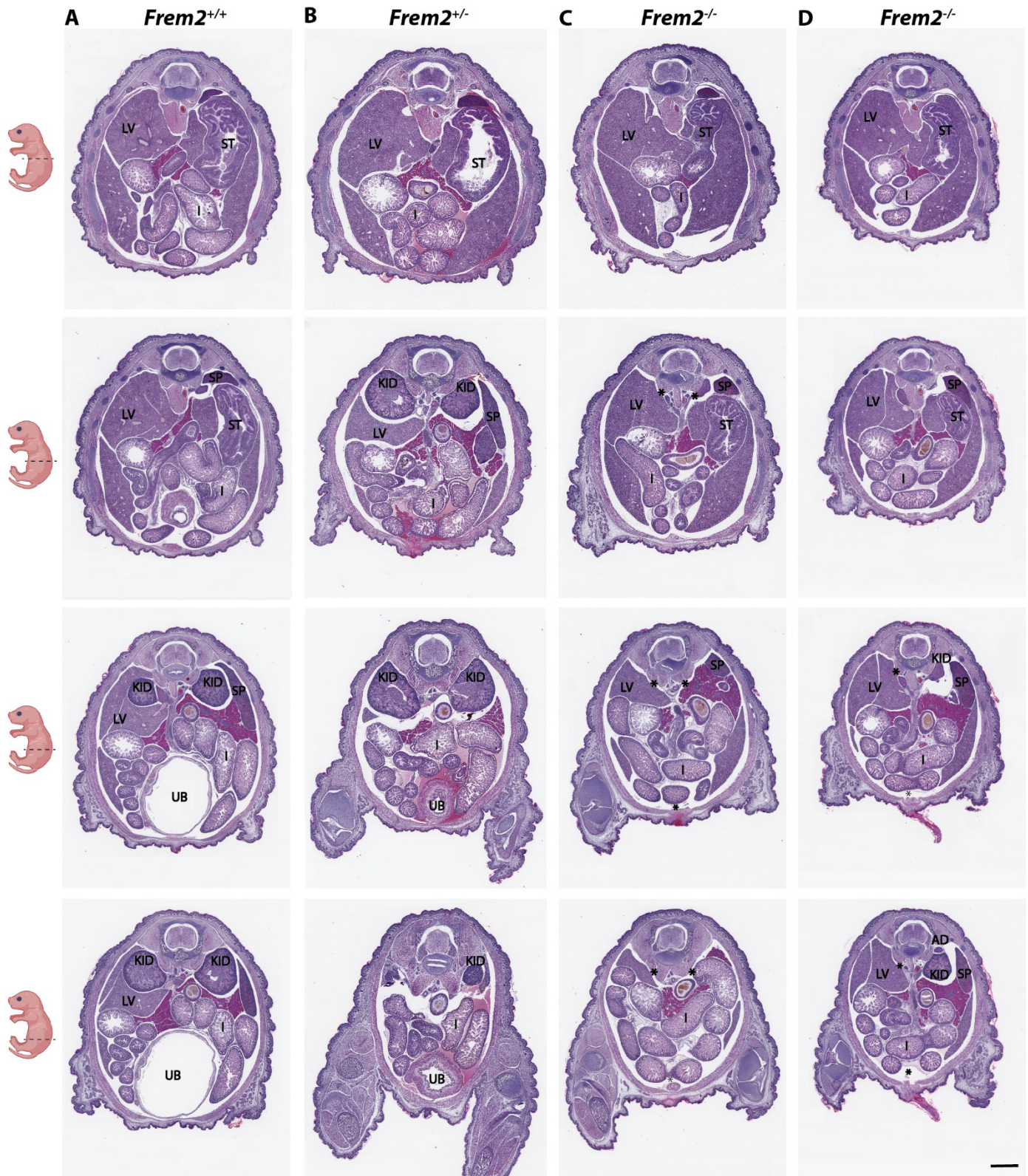


336
 337 **Figure 3. *Frem2*-KO mice lack eyelids and develop blood-filled blisters covering their eyes.** **A**, Gross image of an
 338 E15 *Frem2*^{+/+} fetus with a normal eye, and a *Frem2*^{-/-} fetus (*below*) with a blood-filled blister (*arrowhead*) covering the eye.
 339 **B**, Hematoxylin and eosin-stained coronal head section of a *Frem2*^{+/+} E15 fetus and a higher magnification image below
 340 displays normal eyelid morphology. **C**, Histological section of a *Frem2*^{-/-} E15 fetus with a blood-filled blister and a higher
 341 magnification image displays the absence of the cornea and eyelid. **D**, Low and high magnification histology images of a
 342 *Frem2*^{-/-} E16 fetus with a normal right eyelid and a hemorrhage covering the left eyelid. **E**, Gross images of *Frem2*^{+/+} and
 343 *Frem2*^{-/-} P0 pups show normal eyelids. **F**, Gross images of *Frem2*^{-/-} P0 pups display missing eyelids (*arrowhead*). **G**,
 344 Histology sections of P0 *Frem2*^{+/+} and *Frem2*^{+/+} heads with normal eyelids and their corresponding higher magnification
 345 images of the right (R) and left (L) eyes presented below it. **H**, Histology section of a P0 *Frem2*^{-/-} pup with the thinning of
 346 the eyelid (R) and a missing eyelid with a hemorrhage over the eye (L). **I**, A newborn *Frem2*^{-/-} pup with a missing eyelid (R)
 347 and thinning of the eyelid (L). **J** *Frem2*^{-/-} pup with a missing eyelid (R) and a normal contralateral eyelid (L). Scale bars: (A):
 348 2 mm, (B-G): 1 mm, (H-J): 1 mm.



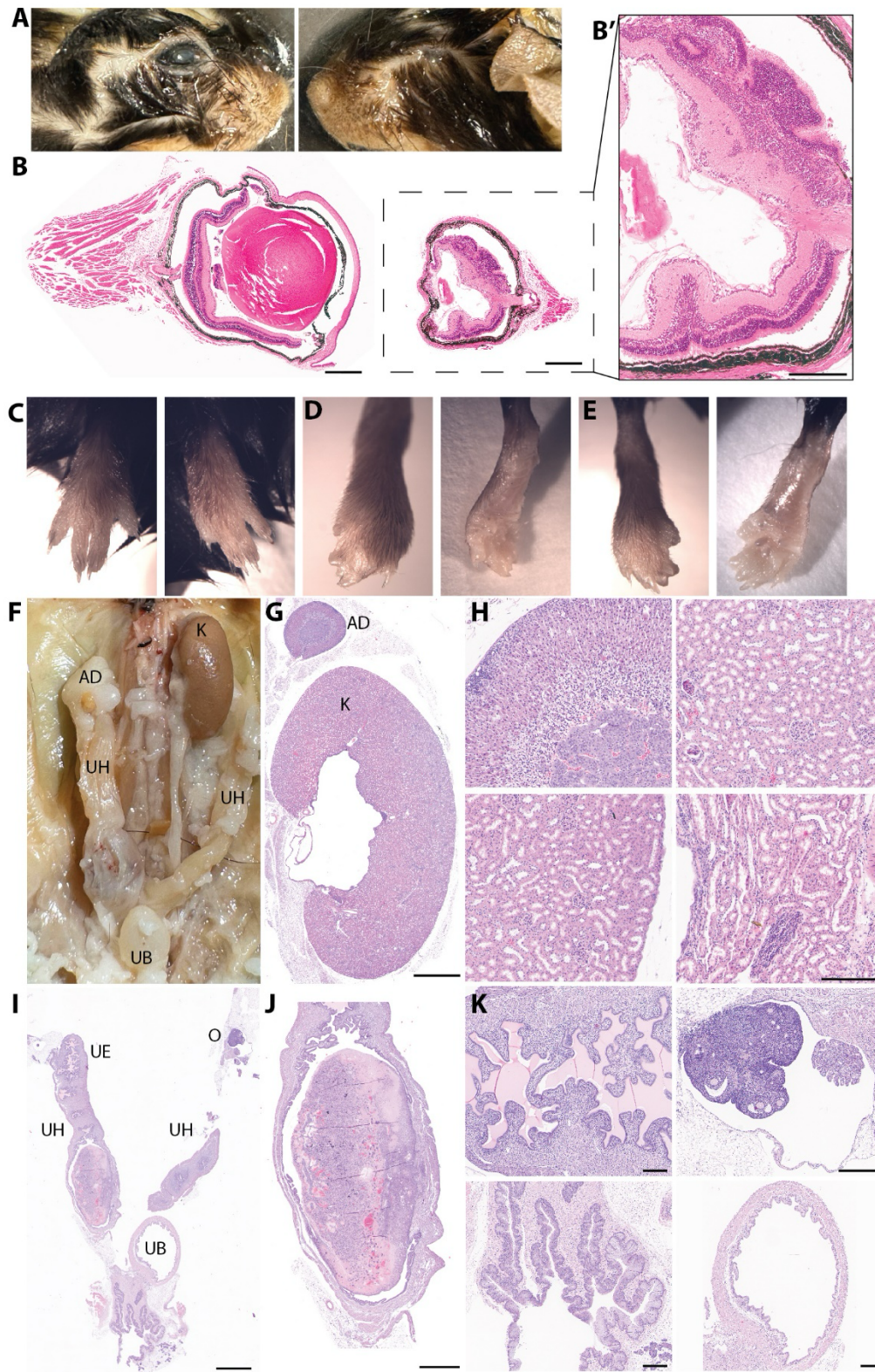
349

350 **Figure 4. Renal agenesis in *Frem2*-KO pups.** Macroscopic images of P0 pups show kidneys (K), adrenal glands (AD),
351 and urinary bladder (UB) present in a *Frem2*^{+/+} pup (A) and kidneys and inconspicuous urinary bladder in a *Frem2*^{-/-} pup (B).
352 Hematoxylin and eosin-stained parasagittal sections of a *Frem2*^{+/+} (left column) and a *Frem2*^{-/-} (right column) P0 pup show
353 organs present to the left (C, D) and right (E, F) of the spinal cord. Locations of the deflated urinary bladders are labeled
354 with asterisks. Sections are from similar regions to compare the presence and morphology of organs. Scale bars: (A, B); 1
355 mm, (C-F); 3 mm. Labels: AD, adrenal glands; K, kidney; H, heart; LV, liver; LUN, lung; I, intestines; S, stomach; UB, urinary
356 bladder.



357

358 **Figure 5. Serial sectioning of newborn (P0) *Frem2* pups reveals renal agenesis in knockout mice.** Sections down the
359 columns progress below the diaphragm to the pelvic region from the same pup. Sections across each row correspond to
360 the same region of each pup's body. Hematoxylin and eosin-stained histology sections from *Frem2*^{+/+} (A) and *Frem2*^{+/-} (B)
361 pups exhibit the presence of both kidneys (KID) and a comparable arrangement of organs. *Frem2*^{-/-} pups display bilateral
362 (C) and unilateral renal agenesis (D). Locations of missing kidneys are labeled with asterisks. Scale bar: (A-D); 1 mm.
363 Labels: AD, adrenal glands; KID, kidney; LV, liver; LUN, lung; I, intestines; SP, spleen; UB, urinary bladder.



364

365 **Figure 6. Characterization of the *Frem2*-KO adult mouse.** (A) Images show the *Frem2*^{-/-} adult mouse with a normal right
366 eye and a left eye affected by cryptophthalmos. (B) Hematoxylin and eosin-stained histology section through the middle of
367 the normal right eye and the defective left eye. The defective left eye reveals the lens with reduced thickness size and retinal
368 dysplasia. (B') Higher magnification image of defective left eye showing microphthalmia. (C) Images of normal front paws
369 and affected right (D) and left (E) hind paws by syndactyly. (F) The gross anatomy image of the adult *Frem2*^{-/-} mouse shows
370 one left kidney (K), adrenal glands (AD), uterine horns (UH), and urinary bladder (UB) present. (G) Histology section of the
371 normal left kidney and adrenal gland. (H) High-magnification images of different regions of the kidney displaying the tubules,
372 collecting ducts, and nephrons. Histology section displays a placental-like tissue (J) in the right uterine horn (I) of the mouse.
373 (K) High-magnification images of the uterine epithelium (UE), ovaries (O), and urinary bladder (UB). Scale bars: (B) 2 mm,
374 (B') 250 μ m, (G) 3 mm, (H) 500 μ m, (I) 4 mm, (J) 2 mm, (K) 250 μ m.

375 REFERENCES

- 376 Alazami, A. M., Shaheen, R., Alzahrani, F., Snape, K., Saggarr, A., Brinkmann, B., Bavi, P., Al-Gazali, L. I., &
377 Alkuraya, F. S. (2009). FREM1 mutations cause bifid nose, renal agenesis, and anorectal malformations
378 syndrome. *American journal of human genetics*, 85(3), 414–418. <https://doi.org/10.1016/j.ajhg.2009.08.010>.
379 PMID: 19732862; PMCID: PMC2771533.
- 380 Anas M. Alazami, Ranad Shaheen, Fatema Alzahrani, Katie Snape, Anand Saggarr, Bernd Brinkmann, Prashant
381 Bavi, Lihadh I. Al-Gazali, Fowzan S. Alkuraya. (2009). FREM1 Mutations Cause Bifid Nose, Renal Agenesis,
382 and Anorectal Malformations Syndrome, *The American Journal of Human Genetics*. Volume 85, Issue 3,
383 Pages 414-418, ISSN 0002-9297, <https://doi.org/10.1016/j.ajhg.2009.08.010>. PMID: 19732862; PMCID:
384 PMC2771533.
- 385 Bladt, F., Tafuri, A., Gelkop, S., Langille, L., & Pawson, T. (2002). Epidermolysis bullosa and embryonic lethality
386 in mice lacking the multi-PDZ domain protein GRIP1. *Proceedings of the National Academy of Sciences*,
387 99(10), 6816-6821. <https://doi.org/10.1073/pnas.092130099>. PMID: 11983858; PMCID: PMC124486.
- 388 Bouaoud, J., Olivetto, M., Testelin, S., Dakpe, S., Bettoni, J., & Devauchelle, B. (2020). Fraser syndrome: review
389 of the literature illustrated by a historical adult case. *International journal of oral and maxillofacial*
390 *surgery*, 49(10), 1245–1253. <https://doi.org/10.1016/j.ijom.2020.01.007>. PMID: 31982235.
- 391 Graw J. (2019). Mouse models for microphthalmia, anophthalmia and cataracts. *Human genetics*, 138(8-9),
392 1007–1018. <https://doi.org/10.1007/s00439-019-01995-w>. PMID: 30919050; PMCID: PMC6710221.
- 393 Ian Smyth , Peter Scambler. (2005) The genetics of Fraser syndrome and the blebs mouse mutants, *Human*
394 *Molecular Genetics*, Volume 14, Issue suppl_2, Pages R269–R274, <https://doi.org/10.1093/hmg/ddi262>.
395 PMID: 16244325.
- 396 Jadeja, S., Smyth, I., Pitera, J. E., Taylor, M. S., van Haelst, M., Bentley, E., McGregor, L., Hopkins, J.,
397 Chalepakis, G., Philip, N., Perez Aytes, A., Watt, F. M., Darling, S. M., Jackson, I., Woolf, A. S., & Scambler,
398 P. J. (2005). Identification of a new gene mutated in Fraser syndrome and mouse myelencephalic blebs.
399 *Nature genetics*, 37(5), 520–525. <https://doi.org/10.1038/ng1549>. PMID: 15838507.
- 400 Kamba T, Higashi S, Kamoto T, Shisa H, Yamada Y, Ogawa O, Hiai H. (2001) Failure of ureteric bud invasion: a
401 new model of renal agenesis in mice. *Am J Pathol*. 159(6):2347-53. doi: 10.1016/S0002-9440(10)63084-2.
402 PMID: 11733383; PMCID: PMC1850611.
- 403 Kerecuk L, Long DA, Ali Z, Anders C, Kolatsi-Joannou M, Scambler PJ, Woolf AS. (2012) Expression of Fraser
404 syndrome genes in normal and polycystic murine kidneys. *Pediatr Nephrol*. 27(6):991-8. doi:
405 10.1007/s00467-012-2100-5. PMID: 21993971; PMCID: PMC3337421.
- 406 Miller JL, Baschat AA, Rosner M, Blumenfeld YJ, Moldenhauer JS, Johnson A, Schenone MH, Zaretsky MV,
407 Chmait RH, Gonzalez JM, Miller RS, Moon-Grady AJ, Bendel-Stenzel E, Keiser AM, Avadhani R, Jelin AC,
408 Davis JM, Warren DS, Hanley DF, Watkins JA, Samuels J, Sugarman J, Atkinson MA. (2023) Neonatal
409 Survival After Serial Amnioinfusions for Bilateral Renal Agenesis: The Renal Anhydramnios Fetal Therapy
410 Trial. *JAMA*. 5;330(21):2096-2105. doi: 10.1001/jama.2023.21153. PMID: 38051327; PMCID:
411 PMC10698620.
- 412 Pavlakis, E., Chiotaki, R., & Chalepakis, G. (2011). The role of Fras1/Frem proteins in the structure and function
413 of basement membrane. *The international journal of biochemistry & cell biology*, 43(4), 487–495.
414 <https://doi.org/10.1016/j.biocel.2010.12.016>. PMID: 21182980
- 415 Pavlakis, E., Makrygiannis, A.K., Chiotaki, R. et al. (2008) Differential localization profile of Fras1/Frem proteins
416 in epithelial basement membranes of newborn and adult mice. *Histochem Cell Biol* 130, 785–793.
417 <https://doi.org/10.1007/s00418-008-0453-4>. PMID: 18563433.
- 418 Petrou, P., Makrygiannis, A. K., & Chalepakis, G. (2008). The Fras1/Frem family of extracellular matrix proteins:
419 structure, function, and association with Fraser syndrome and the mouse bleb phenotype. *Connective tissue*
420 *research*, 49(3), 277–282. <https://doi.org/10.1080/03008200802148025>. PMID: 18661360.
- 421 Short, K., Wiradjaja, F., & Smyth, I. (2007). Let's stick together: the role of the Fras1 and Frem proteins in
422 epidermal adhesion. *IUBMB life*, 59(7), 427–435. <https://doi.org/10.1080/15216540701510581>. PMID:
423 17654118.

- 424 Slavotinek, A. M., & Tiffit, C. J. (2002). Fraser syndrome and cryptophthalmos: review of the diagnostic criteria
425 and evidence for phenotypic modules in complex malformation syndromes. *Journal of medical*
426 *genetics*, 39(9), 623–633. <https://doi.org/10.1136/jmg.39.9.623>. PMID: 12205104; PMCID: PMC1735240.
- 427 Smyth, I., Du, X., Taylor, M. S., Justice, M. J., Beutler, B., & Jackson, I. J. (2004). The extracellular matrix gene
428 *Frem1* is essential for the normal adhesion of the embryonic epidermis. *Proceedings of the National*
429 *Academy of Sciences of the United States of America*, 101(37), 13560–13565.
430 <https://doi.org/10.1073/pnas.0402760101>. PMID: 15345741; PMCID: PMC518794.
- 431 Timmer, J. R., Mak, T. W., Manova, K., Anderson, K. V., & Niswander, L. (2005). Tissue morphogenesis and
432 vascular stability require the *Frem2* protein, product of the mouse myelencephalic blebs gene. *Proceedings*
433 *of the National Academy of Sciences of the United States of America*, 102(33), 11746–11750.
434 <https://doi.org/10.1073/pnas.0505404102>. PMID: 16087869; PMCID: PMC1183448.
- 435 Zhang, X., Wang, R., Wang, T., Zhang, X., Dongye, M., Wang, D., Wang, J., Li, W., Wu, X., Lin, D., & Lin, H.
436 (2021). The Metabolic Reprogramming of *Frem2* Mutant Mice Embryos in Cryptophthalmos Development.
437 *Frontiers in cell and developmental biology*, 8, 625492. <https://doi.org/10.3389/fcell.2020.625492>. PMID:
438 33490088; PMCID: PMC7820765.
- 439

440 SUPPLEMENTAL MATERIALS

441 **Supplemental Movie 1. Serial sectioning of newborn *Frem2^{+/+}* pup 1.** Movie of images from hematoxylin and
442 eosin-stained histology sections from a *Frem2^{+/+}* newborn pup. Transverse sections through the body begin
443 inferior to the front paws and end superior to the hind paws displaying major organs including the lungs, heart,
444 liver, intestines, the urinary bladder, and kidneys. Scale bar: 2 mm

445 **Supplemental Movie 2. Serial sectioning of newborn *Frem2^{+/+}* pup 2.** Movie of images from hematoxylin and
446 eosin-stained histology sections from a *Frem2^{+/+}* newborn pup. Transverse sections through the body begin
447 inferior to the front paws and end superior to the hind paws displaying major organs including the lungs, heart,
448 liver, intestines, the urinary bladder, and kidneys. Scale bar: 2 mm.

449 **Supplemental Movie 3. Serial sectioning of newborn *Frem2^{+/-}* pup 1.** Movie of images from hematoxylin and
450 eosin-stained histology sections from a *Frem2^{+/-}* newborn pup. Transverse sections through the body begin
451 inferior to the front paws and end superior to the hind paws displaying major organs including the lungs, heart,
452 liver, intestines, the urinary bladder, and kidneys. Scale bar: 2 mm.

453 **Supplemental Movie 4. Serial sectioning of newborn *Frem2^{+/-}* pup 2.** Movie of images from hematoxylin and
454 eosin-stained histology sections from a *Frem2^{+/-}* newborn pup. Transverse sections through the body begin
455 inferior to the front paws and end superior to the hind paws displaying major organs including the lungs, heart,
456 liver, intestines, the urinary bladder and kidneys. Scale bar: 2 mm.

457 **Supplemental Movie 5. Serial sectioning of newborn *Frem2^{-/-}* pup 1.** Movie of images from hematoxylin and
458 eosin-stained histology sections from a *Frem2^{-/-}* newborn pup. Transverse sections through the body begin
459 inferior to the front paws and end superior to the hind paws displaying major organs. No urinary bladder can be
460 easily identified and no kidneys are present. Scale bar: 2 mm.

461 **Supplemental Movie 6. Serial sectioning of newborn *Frem2^{-/-}* pup 2.** Movie of images from hematoxylin and
462 eosin-stained histology sections from a *Frem2^{-/-}* newborn pup. Transverse sections through the body begin
463 inferior to the front paws and end superior to the hind paws, displaying all major organs. No urinary bladder can
464 be easily identified and only the left kidney is present. Scale bar: 2 mm.